Remote Sensing Applications: Society and Environment 40 (2025) 101750

Contents lists available at ScienceDirect

Remote Sensing Applications: Society and Environment

journal homepage: www.elsevier.com/locate/rsase

Estimation of aboveground biomass and carbon sequestration in a cocoa agroforestry system using UAV-LiDAR in northwestern Peru

Nilton Atalaya-Marin [a,*], Teiser Sanchez-Fuentes [a], Malluri Goñas [a], Daniel Tineo [a], Victor H. Taboada-Mitma [a], Héctor Cabrera-Hoyos [b], JuanCarlos Cruz-Luis [c], Jorge J. Ganoza-Roncal [c], Darwin Gómez-Fernández [a]

[a] Centro Experimental Yanayacu, Dirección de Servicios Estratégicos Agrarios (DSEA), Instituto Nacional de Innovación Agraria (INIA), Carretera Jaén San Ignacio KM 23.7, Jaén, 06801, Cajamarca, Peru
[b] Estación Experimental Agraria Baños del Inca, Dirección de Servicios Estratégicos Agrarios (DSEA), Instituto Nacional de Innovación Agraria (INIA), Jirón Wiracocha S/N, Cajamarca, 06001, Peru
[c] Dirección de Servicios Estratégicos Agrarios (DSEA), Instituto Nacional de Innovación Agraria (INIA), Av. La Molina 1981, Lima, 15024, Peru

ARTICLE INFO

Keywords:
Agroforestry systems
Climate mitigation
Theobroma cacao L.
Tree segmentation
Sensores remotos

ABSTRACT

Accurate estimation of biomass and carbon in agroforestry systems is essential to assess their contribution to climate change mitigation and to improve their management. In this context, UAV-mounted LiDAR technology emerges as a fast, accurate, and non-destructive alternative for the structural characterization of cocoa agroforestry systems. This study aimed to estimate and analyze structural parameters, mainly tree height and diameter at breast height (DBH), as well as to calculate aboveground biomass and carbon sequestration in a cocoa agroforestry system, using LiDAR data obtained with a DJI Matrice 350 RTK UAV equipped with a Zenmuse L2 sensor, complemented by automatic tree segmentation in LiDAR360 and the application of species-specific allometric equations. The results showed a 93 % segmentation efficiency, with accuracies of 0.93 and 0.99 for DBH and height estimations, respectively. The evaluated plot, located at the Yanayacu Experimental Center (Jaén, Peru) and covering an area of 0.58 ha, had stored 15,492.5 kg of aboveground biomass and 7746.25 kg of aboveground carbon, with *Mangifera indica* and *Cocos nucifera* contributing more than 80 %. Consequently, this approach demonstrates the potential of UAV-based LiDAR to generate accurate and detailed information on system structure, enabling optimized management of high-biomass species and the development of more efficient and sustainable management strategies.

1. Introduction

On the Earth's surface, 78 % of agroforestry is found in tropical regions and 22 % in temperate zones, with Southeast Asia, Central America, and South America being the main areas where agroforestry systems are adopted (Food and Agriculture Organization of the United Nations [FAO], 2025). Among these systems, cocoa agroforestry systems (*Theobroma cacao* L.) are particularly important, as they support approximately 40–50 million people and nearly 5 million households (Löhr et al., 2021). In addition, they contribute to biomass storage (41.3 ± 3.62 Mg/ha) and carbon sequestration (22.9 ± 2.60 Mg/ha), making them a key component in climate change

* Corresponding author. Jaén, 06801, Cajamarca, Peru.
E-mail address: atalayanilton@gmail.com (N. Atalaya-Marin).

https://doi.org/10.1016/j.rsase.2025.101750
Received 9 June 2025; Received in revised form 16 September 2025; Accepted 7 October 2025
Available online 8 October 2025

mitigation and agricultural sustainability (Asigbaase et al., 2021).

Understanding the quantity and distribution of this biomass, and consequently, carbon sequestration, not only allows for the assessment of the productivity and condition of these systems, but also facilitates the economic valuation of forest resources (Hirigoyen et al., 2021). Furthermore, this information supports timber harvesting planning (Pinedo et al., 2025) and helps identify areas with high biomass density that can be prioritized in investment strategies and sustainable development efforts (McRoberts et al., 2019).

The estimation of aboveground biomass in cocoa agroforestry systems faces challenges due to the structural complexity of vegetation and species diversity. Traditionally, this calculation has relied on field inventories in which dendrometric metrics are collected to develop allometric equations for biomass modeling (Goñas et al., 2024). However, obtaining these metrics requires considerable time and resource investment, especially in hard-to-access areas (Zenner and Hibbs, 2000). In addition, traditional approaches largely depend on visual assessments to estimate parameters such as tree height and crown diameter. These estimations, being subject to the observer's perception, introduce variability into the data and affect the accuracy of the calculations (Dantas et al., 2020).

In response to these limitations, remote sensing has emerged as an effective alternative by enabling rapid, detailed, and accurate characterization of vegetation at multiple scales, from individual trees to entire agroforestry systems (Seidel et al., 2021; White et al., 2016). Various technologies are available, including satellite imagery, LiDAR sensors (both terrestrial and airborne), aerial photogrammetry, and hyperspectral and multispectral sensors. These have proven to be valuable tools for estimating biomass and carbon without the need for destructive field measurements (Fadil et al., 2024).

LiDAR technology, in particular, has proven to be highly effective for this purpose and has recently transitioned from a demonstration tool to an essential instrument for assessing carbon stocks (Asner et al., 2012). This technology has modernized the way these systems are observed by enabling the acquisition of previously inaccessible information about their three-dimensional structure, thereby facilitating more accurate estimates of aboveground biomass and, consequently, carbon storage (Haneda et al., 2025).

There are two main approaches in the application of LiDAR: terrestrial and airborne. Terrestrial LiDAR has been used to assess structure, biomass, and carbon sequestration in cocoa agroforestry systems, achieving high levels of accuracy ($R^2 = 0.98$) (Momo et al., 2018). However, its application faces limitations due to the time required for scanning and the logistical challenges of transporting the equipment within the plots (Momo et al., 2018; Peynaud and Momo, 2024).

Airborne LiDAR, on the other hand, has overcome these limitations by offering a more efficient and operationally viable alternative (Vaglio et al., 2016). Its ability to capture detailed three-dimensional data on forest structure (Almeida et al., 2021) reduces the need for extensive field campaigns, optimizing data collection in hard-to-reach areas quickly and at lower cost. In addition, it enables the detection of up to 82 % of tree stems (Neuville et al., 2021), which supports the development of accurate models for biomass prediction (Duncanson et al., 2022).

Despite its advantages, the application of LiDAR technology for biomass estimation in cocoa agroforestry systems in Peru has not yet been documented, revealing a significant knowledge gap. Therefore, the aim of this study was to estimate and analyze the

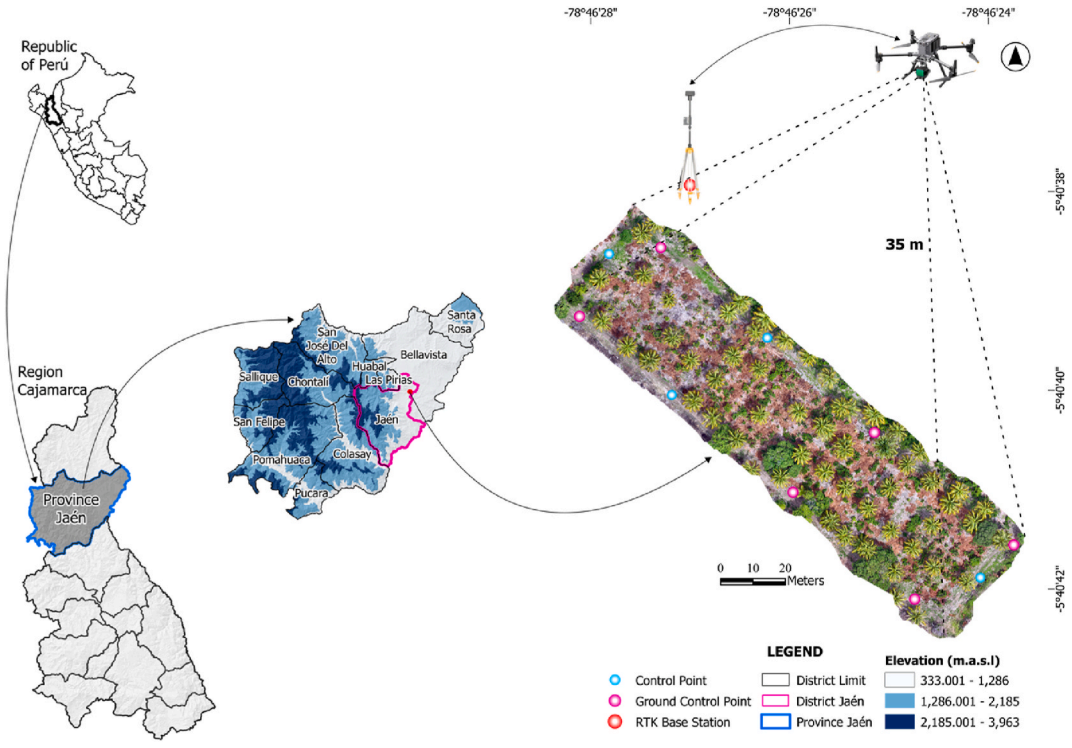

Fig. 1. Geographic location and delimitation of the study area, including representation of the experimental site and control points.

structural parameters of a cocoa agroforestry system, as well as to calculate aboveground biomass and carbon sequestration for all trees using automatic segmentation based on LiDAR data acquired with a UAV.

2. Materials and methods

2.1. Study area

The study was conducted in a *T. cacao* L. agroforestry system located within the clonal garden of the Yanayacu Experimental Center, part of the National Institute of Agricultural Innovation (INIA), in the city of Jaén, Perú (5°40′40.30″ S, 78°46′26.09″). The plot has a predominantly flat topography and is situated at an elevation between 614 and 620 m above sea level. The local climate is semi-dry, warm, and humid throughout the year, with average temperatures ranging from 29 to 33 °C and annual precipitation between 900 and 1200 mm (Servicio Nacional de Meteorología e Hidrología del Perú [SENAMHI] 2020). The predominant soils are Fluvisols and Phaeozems, formed from fluvio-alluvial deposits (Gobierno Regional de Cajamarca [GRC], 2012), with a soil organic carbon content of 31.9 g/kg (Poggio et al., 2021). The study area covers 0.58 ha and contains a diversity of tree species, including *C. nucifera*, *M. indica*, *Averrhoa carambola*, *Cedrela odorata*, and *Persea americana* (Fig. 1).

2.2. Methodological flow

The methodology of this research was structured in the following stages: data acquisition (a), data processing (b), and biomass and carbon stock modeling (c) (Fig. 2).

2.2.1. Data acquisition

Data acquisition was carried out in two phases. The first was an exploratory phase using a Mavic 3 Enterprise RTK unmanned aerial vehicle (UAV) to delineate the plot boundary, establish six Ground Control Points (GCP), four Check Points (CP), and one base point (Fig. 1), all georeferenced with a South Galaxy G7 GNSS receiver. These points were later used to adjust the point cloud, the generated orthophoto, and to obtain the accuracy report. The second phase involved data collection using a DJI Matrice 350 RTK UAV equipped with the DJI Zenmuse L2 sensor, which features a horizontal accuracy of 5 cm and a vertical accuracy of 4 cm, an effective range of 250 m, and a point acquisition rate of 240,000 points per second.

The LiDAR survey was planned using UGCS 5.8.2 software, applying a double grid pattern and configuring two camera angles (−90° and −45°) to increase point density. The flight was conducted at an altitude of 35 m above ground level, with a speed of 3.5 m/s and a lateral and frontal overlap of 70 % (Fig. 3a).

Additionally, all trees within the *T. cacao* L. agroforestry system were georeferenced and recorded using a South G7 receiver, totaling 392 individuals. From this population, the sample size was calculated with a 90 % confidence level and a 10 % margin of error, resulting in 59 trees; for practical reasons, the number was rounded to 60 individuals to ensure representativeness. The sample consisted of 30 cocoa trees (50.0 %) and 30 accompanying species, randomly selected in QGIS using the Random selection tool from the Vector/Research menu (Fig. 3b). As a result of this random selection, the accompanying species corresponded to *C. nucifera* (29 individuals, 48.3 %) and *C. odorata* (1 individual, 1.7 %). For each tree, the circumference at breast height (CBH) was measured with a

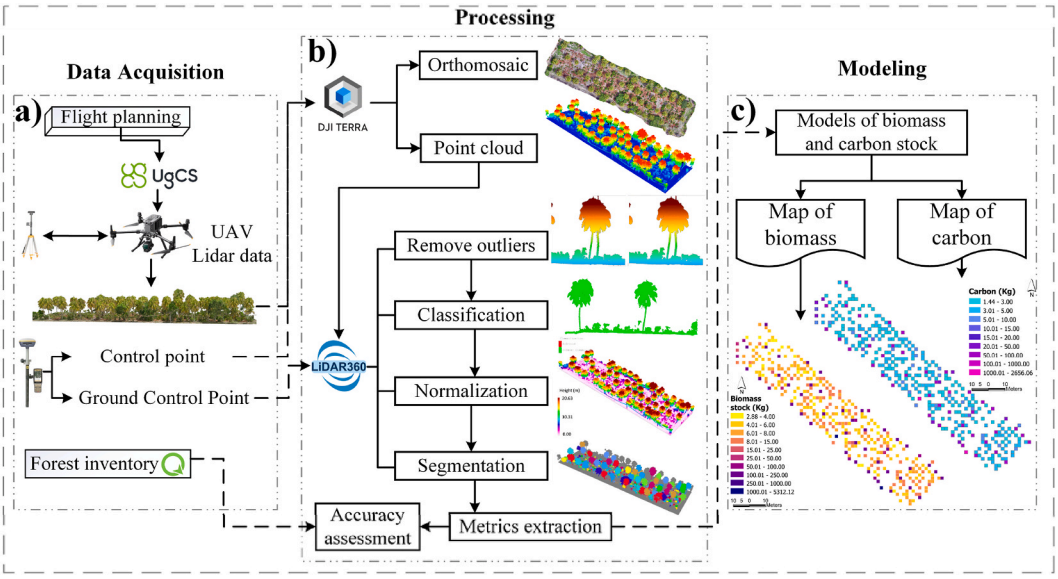

Fig. 2. Flowchart of the methodological process for biomass and carbon estimation using UAV LiDAR data.

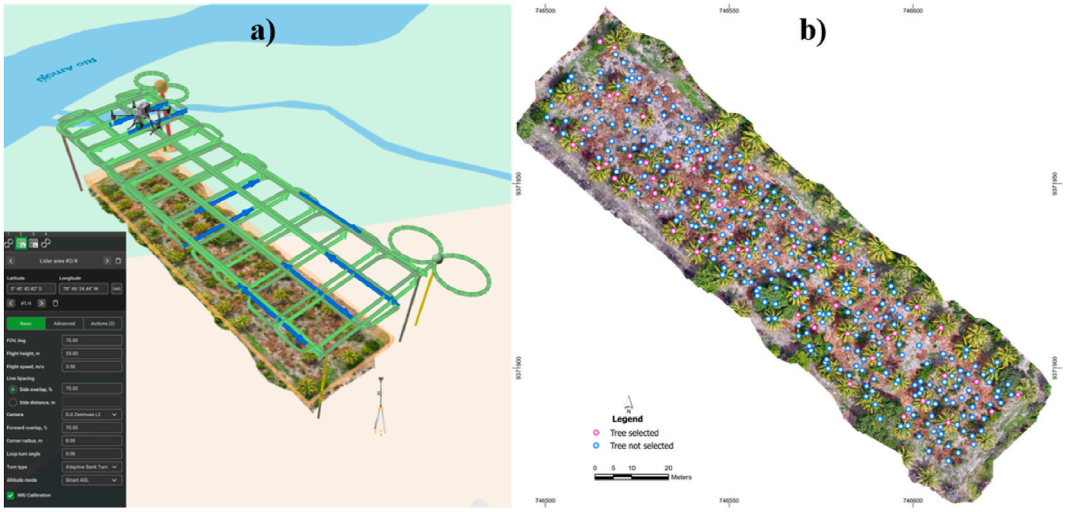

Fig. 3. Collection of Structural Data: a) LiDAR flight planning with double grid and camera angles; b) field measurement of tree height and CBH in 60 trees to validate the segmentation.

2-m Huiiley® retractable tape, and total height was determined with a Nikon Forestry Pro II hypsometer (range: 1600 m; resolution: 0.1 m; accuracy: ±0.3 m < 1000 m, ±1.0 m > 1000 m). These field measurements were subsequently used to validate the structural attributes extracted after the segmentation process.

2.2.2. *Processing*

2.2.2.1. Generation of orthomosaic and LiDAR point cloud. The data acquired using the DJI Zenmuse L2 sensor were processed with DJI Terra 4.5.0 software, integrating six Ground Control Points (GCP) to ensure accurate georeferencing. As a result, two products were generated: an RGB-based orthomosaic (Fig. 4a) and a LiDAR point cloud colored according to the RGB images collected during the flight (Fig. 4b–d).

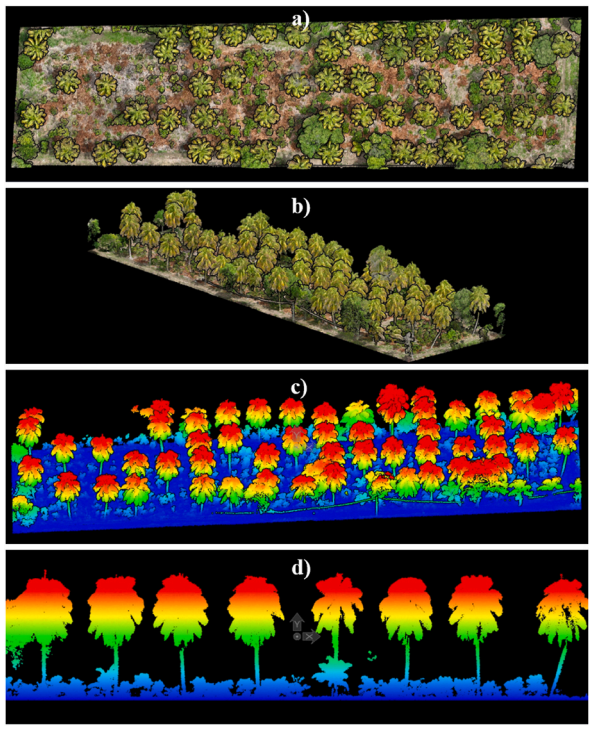

Fig. 4. Visualization of the products generated with DJI Terra: a) 2D Orthomosaic; b–d) 3D LiDAR Point Cloud.

2.2.2.2. LiDAR point cloud processing. The point cloud generated in DJI Terra 4.5.0 was imported into the post-processing software LiDAR 360 version 8.2, where the accuracy of the results was evaluated using four points different from the six GCPs used during point cloud generation (Fig. 1). Outliers were then removed using the Outlier Removal tool (Fig. 5a and b) to optimize the quality of the processed data (Ning et al., 2018). Subsequently, points were classified using the Classify Ground Points tool, allowing the distinction between ground points and above-ground or vegetation points (Fig. 5c) (Zhao et al., 2016).

To minimize the impact of topographic relief on elevation data, the point cloud was normalized by subtracting the ground elevation from the Z-value of each point. As shown in Fig. 6a, before normalization, the elevations were referenced to sea level. After the process, as illustrated in Fig. 6b, the data reflected only the relative height of objects above the ground surface (Fadil et al., 2024).

2.2.2.3. Segmentation and extraction of UAV LiDAR metrics. Once the points were normalized, tree segmentation was performed using the Point Cloud Segmentation tool, configuring the parameters based on optimal results and considering the data collected during the exploratory phase: Cluster Tolerance (0.3), Minimum Cluster Size (500), Minimum DBH (0.05 m), Maximum DBH (0.95 m), Height Above Ground (0.5 m), Minimum Tree Height (2 m), and Trunk Height (1.5 m). The Individual Tree Editor tool was then used to manually refine the segmentation in cases where errors were detected. Finally, individual tree parameters such as coordinates, total height, DBH, crown area, crown volume, and others were extracted and exported in CSV format for subsequent integration and analysis in ArcGIS Pro 3.1.0.

2.2.3. Modeling

Biomass calculation was conducted in several stages. First, the data obtained in CSV format from LiDAR 360 were imported into ArcGIS Pro 3.1.0 and converted into a point shapefile (.shp). Then, species were classified based on their height, distinguishing *T. cacao* L. (<6 m) from other species (>6 m). For the identification of additional species, information collected during fieldwork, the overlay of points on the previously generated RGB mosaic, and inspection of the point cloud in LiDAR 360 were used in cases where species identity was uncertain.

Finally, biomass was calculated by applying species-specific allometric equations, as detailed in Table 1. The resulting biomass values were then multiplied by the carbon fraction (0.5) (McGroddy et al., 2004) to obtain the amount of sequestered carbon.

Where: AGB (kg) = Aboveground biomass; DBH (cm) = Diameter at breast height; H (m) = Height.

2.2.4. Evaluation of the accuracy

The evaluation of automatic tree segmentation performed in LiDAR 360 was based on two approaches: (i) the overall accuracy in detecting individual trees, and (ii) the accuracy of the estimated structural metrics (height and DBH).

For the first approach, the percentage of correctly segmented trees was calculated in relation to the total number of georeferenced individuals in the field. This overall accuracy was estimated using Equation (1):

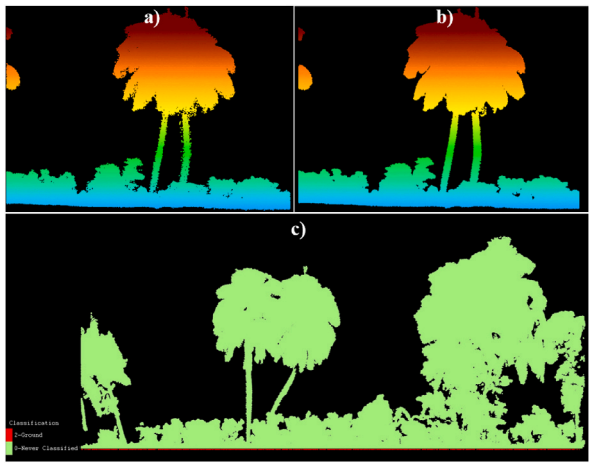

Fig. 5. Filtering and classification of the point cloud in LiDAR 360: (a–b) outlier removal; (c) ground and vegetation classification.

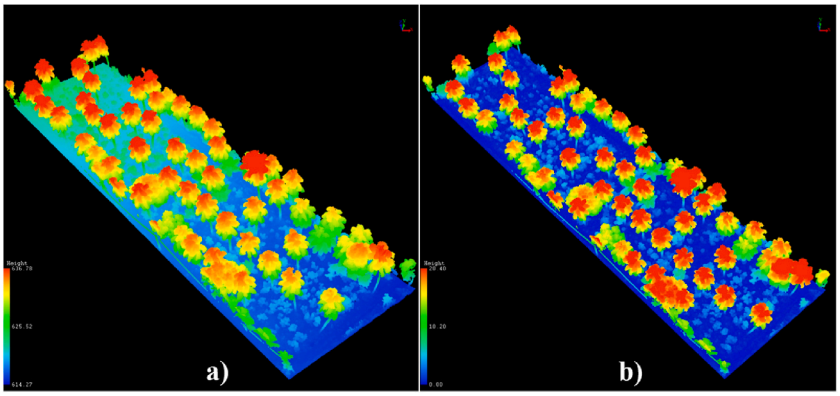

Fig. 6. (a) Point cloud visualization before normalization; (b) point cloud visualization after normalization.

Table 1
Allometric equations used for the calculation of aboveground biomass by species.

Species	Equation	R2	Reference
T. cacao L.	$AGB = EXP - 1.501 + 0.69*LN(DBH^2*H)$	0.937	Fomekong et al. (2024)
C. nucifera	$AGB = 4.5 + 7.7*H$	0.90	Anguiano et al. (2013)
P. americana	$AGB = 0.0446*DBH^{2.3236}*H^{0.4506}$	0.92	Kuyah et al. (2024)
M. indica	$AGB = EXP(-2.7518 + 242*LN(DAP) + 0.49*LN(H)$	0.96	Miah et al. (2020)
C. alliodora	$AGB = 10^{(-0.51+2.08*\log(DBH))}$	0.92	Andrade et al. (2008)
A. carambola	$AGB = 10^{(-1.11+2.64*Log(DBH))}$	0.95	Andrade et al. (2008)
C. Odorata	$AGB = 0.00341*DBH^{3.38248}$	0.978	Benavides-Solrio et al. (2021)

$$\text{Accuracy}\ (\%) = \left(\frac{\text{Segmented trees}}{\text{Georeferenced field trees}}\right)*100 \quad \text{Equation 1}$$

For the second approach, a field dataset corresponding to 60 randomly selected trees (Fig. 3b) was used. Based on these measurements, a comparison matrix was constructed between the estimated and actual values. This matrix was used to calculate four error metrics: mean absolute error (MAE), root mean square error (RMSE), coefficient of determination (R^2), and the concordance index (d), according to Equations (2)–(5):

$$MAE = \frac{1}{n}\sum_{i=1}^{n}|y_i - \hat{y}_i| \quad \text{Equation 2}$$

$$RMSE = \sqrt{\frac{1}{n}\sum_{i=1}^{n}(y_i - \hat{y}_i)^2} \quad \text{Equation 3}$$

$$R^2 = 1 - \frac{\sum_{i=1}^{n}(y_i - \hat{y}_i)^2}{\sum_{i=1}^{n}(y_i - \bar{y})^2} \quad \text{Equation 4}$$

$$d = 1 - \frac{\sum_{i=1}^{n}(y_i - \hat{y}_i)^2}{\sum_{i=1}^{n}(|y_i - \bar{y}| + |y_i - \bar{y}|)^2} \quad \text{Equation 5}$$

Where: y_i = observed value; $\hat{y}_i$ = estimated or predicted value; $\bar{y}$ = mean of the observed values; n = total number of observations.

These error metrics were calculated based on the mathematical formulations of Equations (2)–(5), employing the Python programming language (v.3.10) within the Google Colaboratory environment. The libraries NumPy (v.2.0.2) and scikit-learn (v.1.6.1) were used for the estimation of error metrics, while pandas (v.2.2.2) supported data management and Matplotlib (v.3.10.0) together with Seaborn (v.0.13.2) were applied for graphical visualization. This workflow ensured methodological transparency and the reproducibility of the statistical analyses.

3. Results

3.1. Individual tree segmentation

The automatic tree segmentation performed in the LiDAR 360 post-processing software enabled the identification of 7 tree species, with a total of 368 individuals out of the 392 georeferenced in the field, achieving an accuracy of 93.88 % (Fig. 7). Most of the undetected trees were located beneath dense canopies, which partially limited their detection.

Regarding species composition, *T. cacao* L. was the dominant species, representing 84.2 % of the total individuals (n = 310). *C. nucifera* was the second most abundant species, with 50 individuals (13.6 %), while *A. carambola*, *M. indica*, *C. alliodora, C. odorata*, and *P. americana* each had fewer than three individuals (Fig. 8).

3.2. Metric extraction

The automatic extraction of structural metrics enabled the analysis of relationships among structural variables for 368 segmented trees. A strong relationship was observed between DBH and crown volume ($R^2 = 0.84$), as well as with crown area ($R^2 = 0.81$). Tree height showed a high correlation with average crown diameter ($R^2 = 0.81$) and DBH ($R^2 = 0.80$). Likewise, crown diameters measured in different directions exhibited a strong correlation ($R^2 = 0.90$) (Fig. 9).

3.2.1. Coefficient of determination in height estimation

The LiDAR 360 software generates multiple structural metrics of vegetation (Fig. 9). To evaluate the accuracy of automatic tree height estimation, the values generated through segmentation were compared with field measurements taken from 60 individual trees. The results show a high level of agreement, although a slight deviation and dispersion were observed between both data sources. A coefficient of determination ($R^2 = 0.996$), mean absolute error (MAE = 0.28 m), root mean square error (RMSE = 0.43 m), and concordance index (d = 0.999) were obtained. These indicators confirm the reliability of the applied methodology (Fig. 10).

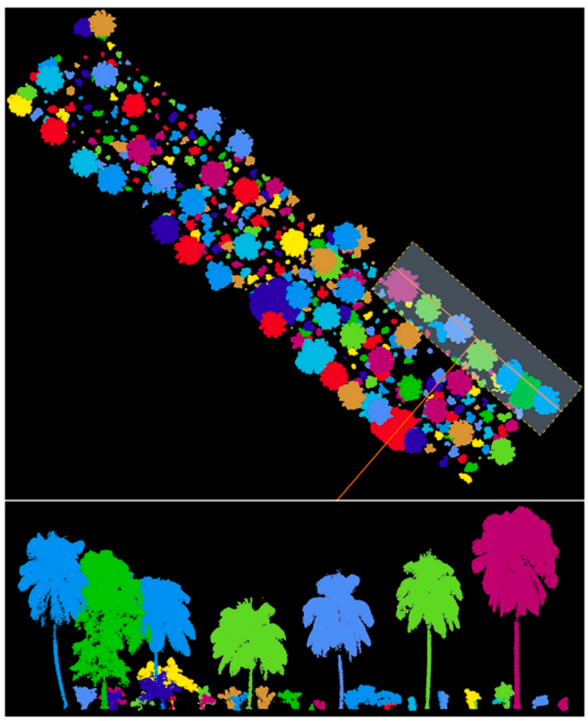

Fig. 7. Results of automatic tree segmentation in LiDAR 360.

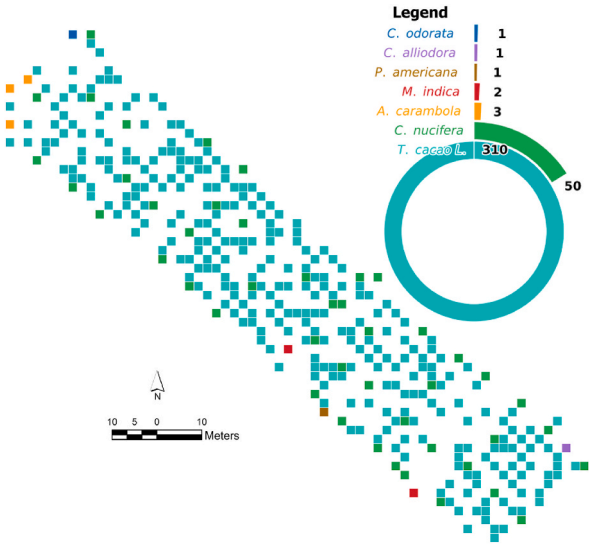

Fig. 8. Distribution of tree species identified through segmentation in LiDAR 360.

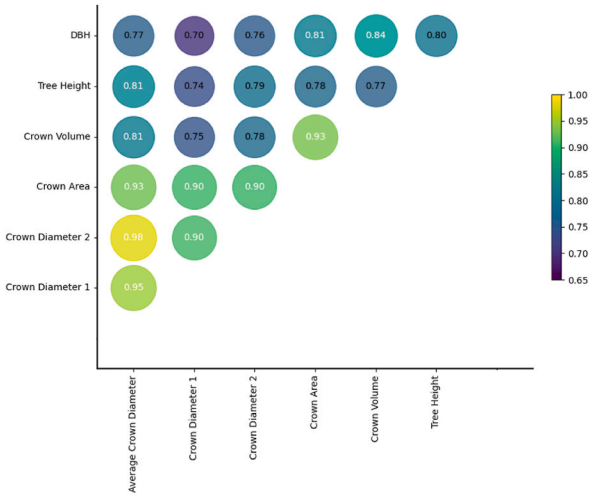

Fig. 9. Correlation matrix of structural metrics obtained with LiDAR 360 in a cocoa agroforestry system.

3.2.2. Coefficient of determination in diameter at breast height (DBH) estimation

Regarding DBH, the results showed a solid agreement with field measurements, with a coefficient of determination of $R^2 = 0.895$, a mean absolute error (MAE) of 3.19 cm, and a root mean square error (RMSE) of 4.30 cm. In addition, the concordance index reached a value of $d = 0.932$, although the dispersion of the values was more evident in diameters greater than 20 cm (Fig. 11).

3.3. Biomass and carbon storage estimation using UAV-LiDAR

Biomass estimation in the cocoa agroforestry plot was carried out by applying species-specific allometric regressions and using automatically extracted metrics for each individual tree. The results show that the system stores 15,492.5 kg of aboveground biomass, with *M. indica* being the species with the highest biomass concentration (47.7 %, 7392.8 kg), followed by *C. nucifera* (36.6 %, 5562.7 kg) and *T. cacao* L. (13.2 %, 2043.1 kg). Other species, such as *A. carambola*, *C. alliodora*, *C. odorata*, and *P. americana*, contribute less, mainly due to their lower abundance within the plot.

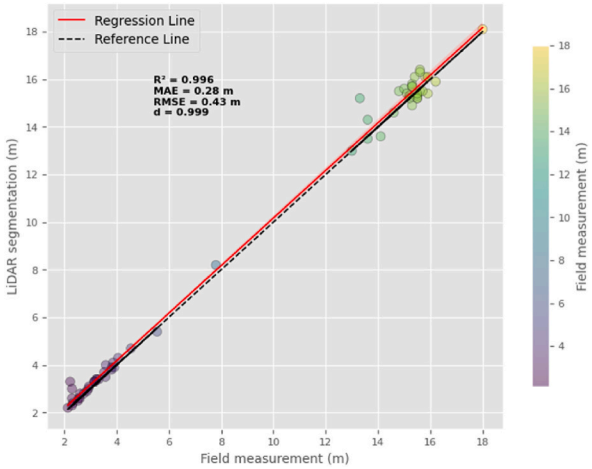

Fig. 10. Relationship between tree height estimated with LiDAR 360 and field measurements.

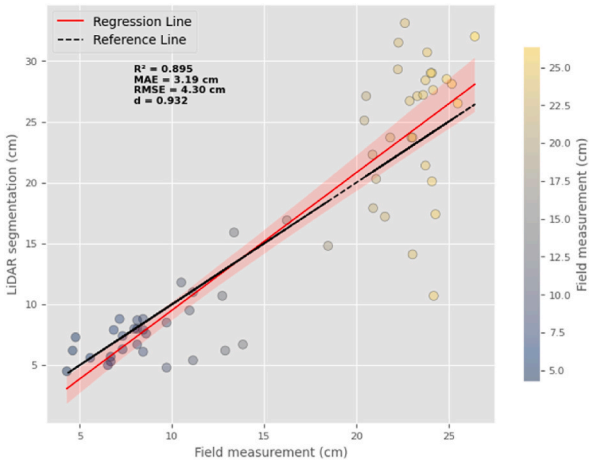

Fig. 11. Relationship between diameter at breast height (DBH) estimated with LiDAR 360 and field measurements.

Spatially, biomass is mostly concentrated along the plot boundary and in the southwestern section, while significantly lower values are observed in the northwestern area, correlating with lower vegetation density. Carbon storage follows a similar pattern, with 7746.25 kg of aboveground carbon stored. *M. indica* accounts for the highest share (47.7 %, 3696.4 kg-C), followed by *C. nucifera* (36.6 %, 2831.4 kg-C) and *T. cacao* L. (13.2 %, 1021.6 kg-C). In contrast, *C. odorata* had the lowest carbon storage (0.05 %, 3.5 kg-C).

These results highlight the importance of species with greater volume and diameter in biomass and carbon accumulation within the agroforestry system, emphasizing the role of *M. indica* and *C. nucifera* in carbon capture and storage (Fig. 12).

To provide a concise comparison of the structural attributes and biomass allocation across species, Table 2 summarizes the number of individuals, mean DBH, tree height, average biomass and carbon values, together with the statistical validation metrics (R^2, MAE, RMSE, d) for UAV-LiDAR estimates of tree height and DBH.

4. Discussion

4.1. Tree segmentation

Automatic tree segmentation using UAV-LiDAR data proved to be an effective tool for identifying individual trees in cocoa agroforestry systems, achieving an accuracy exceeding 93 %. Although few studies have focused on this objective, Peynaud & Momo (2024) reported the identification of 55 individual cocoa trees using terrestrial LiDAR in 30 min. In contrast, this study successfully

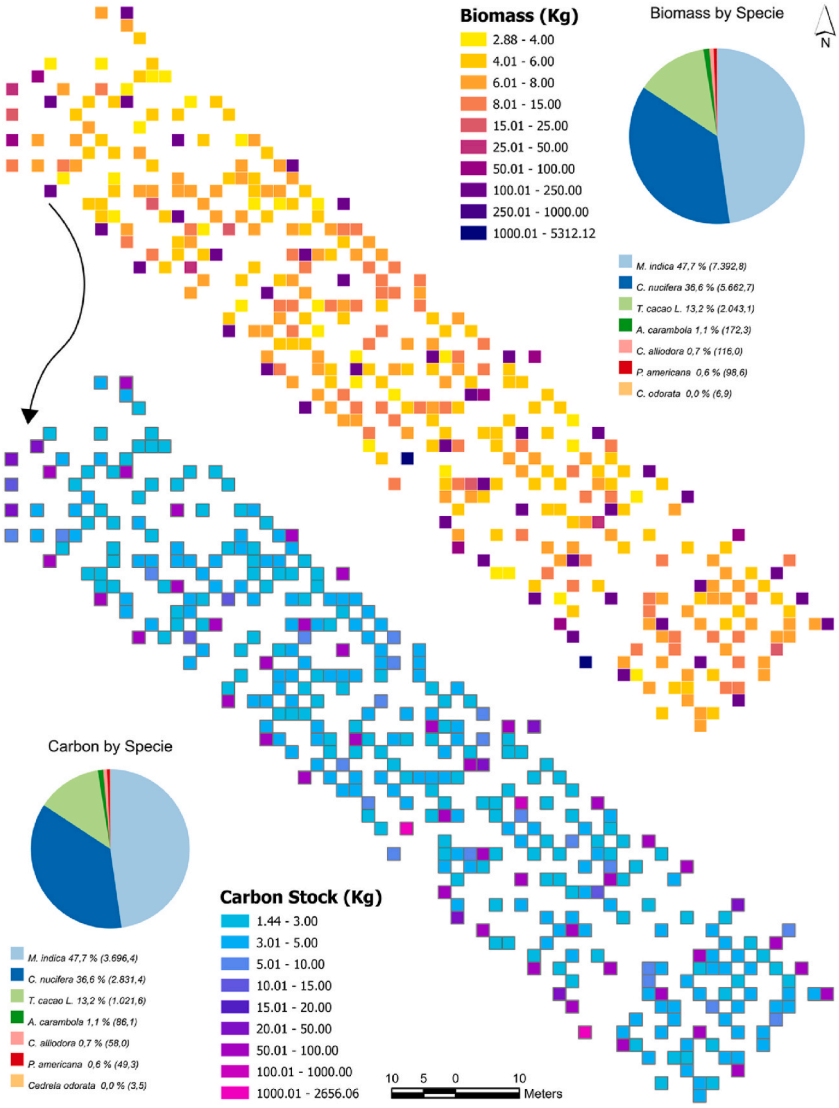

Fig. 12. Spatial distribution of biomass and carbon storage in a cocoa agroforestry system using UAV-LiDAR.

Table 2
Summary of statistical metrics by species and validation of UAV-LiDAR estimates of tree height and DBH.

Species		Mean			
	Plants (n)	DBH (m)	Height (m)	Biomass (kg)	Carbon (kg)
T. cacao L.	310	0.244	2.407	6.591	3.295
A. carambola L.	3	0.3	5.467	57.423	28.712
C. odorata L.	1	0.095	8.2	6.916	3.458
C. nucifera L.	50	0.218	14.124	113.255	56.627
C. alliodora	1	0.449	16.2	116.022	58.011
M. indica L.	2	0.5	14.35	3696.42	1848.21
P. americana	1	0.04	11.6	98.597	49.298
Validation					
	Plants (n)	R^2	MAE (m)	RMSE (m)	d
Tree height	60	0.996	0.28	0.43	0.999
DBH	60	0.895	0.0319	0.043	0.932

segmented 368 trees using UAV-LiDAR in the same amount of time, demonstrating that it is a more efficient and faster alternative for monitoring complex agroforestry systems.

However, achieving 100 % segmentation remains a challenge due to the high heterogeneity of these systems, where up to 49 associated species may coexist (Atalaya-Marin et al., 2025). In our case, although only 7 species were identified, the evaluated plot has been established for over 25 years, resulting in a dense and overlapping canopy. This condition, along with the morphological variability of the species, made automatic segmentation more difficult compared to more homogeneous systems, such as Pinus and Eucalyptus plantations, where higher accuracies have been reported—up to 0.96 for Pinus (Jarahizadeh and Salehi, 2025) and averages above 0.97 for Eucalyptus (Deng et al., 2024). This highlights that the structural complexity of cocoa agroforestry systems continues to pose a limitation for automatic segmentation processes.

4.2. Structural metrics

By correlating all automatically obtained structural metrics, consistent relationships were identified ($R^2 > 0.7$) between DBH, tree height, and crown variables (Fig. 9). These patterns indicate that more robust trees tend to develop broader and more voluminous crowns, which is particularly useful in high-density forest contexts where direct DBH estimation may be limited.

Previous studies have shown that it is possible to model DBH using the most accessible and accurate structural metrics (Jucker et al., 2017). In addition, strong allometric relationships exist between DBH, height, crown dimensions, and even biomass (Pinedo et al., 2025), which reinforces the applicability of these metrics in the structural and functional monitoring of forest ecosystems (Silva et al., 2016).

4.3. Height and DBH estimation

In this study, tree height estimation using UAV-based LiDAR showed a high level of agreement with field measurements ($R^2 = 0.998$, Fig. 10), demonstrating that the flight strategy based on a double grid and two camera angles (Fig. 3a) enabled precise characterization of the vertical structure.

Although surveys integrating both configurations have not been previously documented, other studies have reported similar results, though with lower accuracy. For example, a study conducted in a silvopastoral system characterized by low crown density achieved an R^2 of 0.97 (Clark et al., 2004).

However, in denser formations such as forests, accuracy can decrease to $R^2 = 0.85$ Schimalski et al. (2024), $R^2 = 0.77$ Pinedo et al. (2025), and $R^2 = 0.73$ Thinley et al. (2025). These scenarios highlight the importance of properly adjusting parameters such as flight altitude, camera angle, and grid design to ensure high point density and accurate tree height estimation in complex systems, while also considering that strong winds may affect accuracy.

Regarding diameter at breast height (DBH) estimation, an acceptable correlation was obtained with field data, although slightly lower than that recorded for total height ($R^2 = 0.895$). The decrease in accuracy was mainly observed in trees with diameters greater than 20 cm (Fig. 11), which is attributed to the LiDAR sensor's limited ability to penetrate dense canopies and fully capture the mid-trunk geometry (Fig. 13). Similar results were reported by Cao et al. (2019), with an accuracy of $R^2 = 0.72$. However, studies that combined airborne and terrestrial LiDAR data significantly improved DBH estimation, achieving near-exact values ($R^2 = 0.99$) due to the higher point density in the middle section of the stem (Tantrairatn et al., 2025).

These results confirm that point density particularly in the middle section of the trunk is a key factor in improving the accuracy of DBH estimation. However, for large areas, it is recommended to adjust the data acquisition resolution by balancing information quality with storage and processing capacity, which are the main operational limitations when managing large volumes of LiDAR data (Béjar-Martos et al., 2022).

Fig. 13. Comparison of Canopy Density Effects on LiDAR Point Capture of the Trunk: (a) Dense canopy limiting point capture on the trunk; (b) Lower canopy density enabling greater definition and trunk registration.

4.4. Biomass and carbon

The biomass and carbon estimation showed that species such as *M. indica* and *C. nucifera* accounted for more than 80 % of the total stored in the cocoa agroforestry plot (Fig. 13). Similarly, Asigbaase et al. (2021) reported that in their study plots, a small group of shade species contributed over 70 % of the accumulated carbon, positioning *T. cacao* L. as a secondary species in terms of biomass, despite being the main crop.

Likewise, recent research has concluded that cocoa agroforestry systems can capture up to six times more carbon than monocultures (Rajab et al., 2016), highlighting the functional role of shade species in carbon dynamics.

When comparing with other ecosystems, it is observed that the effectiveness of LiDAR for estimating biomass and carbon depends on structural complexity. In homogeneous birch stands, Fedorov et al. (2023) reported minimal errors (0.2–6.8 %) with UAV-LiDAR. In coniferous forests, Su et al. (2023) improved carbon estimation through the integration of LiDAR, multispectral indices, and field data ($R^2 = 0.903$). Complementarily, Su et al. (2024) reached up to 95 % accuracy by combining backpack LiDAR with multispectral imagery in Larix gmelinii and Betula platyphylla forests. Even in more heterogeneous contexts, Oliveira et al. (2021) confirmed the usefulness of LiDAR for modeling biomass and carbon. Altogether, this evidence explains that the heterogeneity of cocoa agroforestry systems increases the difficulty of estimation; however, the results of this study confirm that UAV-LiDAR maintains solid and applicable performance in diverse agroecosystems.

4.5. Limitations and practical implications

However, accurately estimating the actual amount of biomass and carbon still requires further study. Even when calculations are performed by species and specific algorithms are applied, results may vary depending on local conditions. Although this study employed species-specific allometric equations with coefficients of determination greater than $R^2 > 0.90$ (Table 1), these equations may underestimate actual values, as they were not developed specifically for this region (Ketterings et al., 2001). Nevertheless, this approach is more feasible compared to developing local allometric equations through destructive validation, as it avoids compromising natural regeneration and helps preserve ecosystem integrity (Pati et al., 2022).

Among the limitations, in addition to the reliance on pre-existing allometric equations, operational factors such as LiDAR sensor resolution, point density, weather conditions during the flight, and canopy cover influenced the accuracy of the metrics obtained. Likewise, the absence of an explicit uncertainty analysis restricted the definition of confidence intervals for carbon estimates. Although the field sample of 60 trees was statistically calculated and distributed to ensure representativeness within the plot, future studies could expand the number of individuals, include additional plots, and consider all species present in the system to increase the capacity for generalization. Furthermore, the lack of destructive field validation limited the possibility of directly confirming biomass and carbon estimates with observed values, which would have provided greater certainty regarding the accuracy of the model.

Despite these constraints, the results reaffirm the value of UAV-mounted LiDAR as an innovative, accurate, and non-destructive tool for structural monitoring and carbon estimation in cocoa agroforestry systems. Its application enables high-resolution capture of structural characteristics, contributing to a deeper understanding of the role of companion species in carbon dynamics. Furthermore, this approach allows for plot management to be guided by objective information, supporting decisions such as conserving or propagating species that contribute most to carbon capture, intervening in areas with lower biomass density, reorganizing tree arrangement to improve system efficiency, and adjusting management practices based on the actual structure of vegetation. In this way, climate change mitigation efforts are strengthened from an agroecological perspective without relying on invasive or destructive methods.

5. Conclusions

The implementation of LiDAR technology mounted on unmanned aerial vehicles proved to be an effective tool for the detailed structural analysis of cocoa agroforestry systems. This methodology enabled precise and automated vegetation characterization, facilitating the extraction of structural metrics at the individual tree level. Moreover, it demonstrated strong potential for describing the spatial configuration of the system and establishing consistent structural relationships, reinforcing its applicability in agroforestry monitoring, management, and planning with greater precision.

In addition, the use of species-specific allometric equations applied to automatically extracted metrics allowed for non-destructive estimation of aboveground biomass and carbon with high accuracy. Although equations with coefficients of determination greater than $R^2 > 0.90$ were used, potential biases are acknowledged due to their development outside the study area. Nevertheless, this methodology offers a practical and sustainable alternative to destructive methods, enabling more reliable carbon estimates and supporting more efficient planning in cocoa agroforestry systems.

In conclusion, the strength of this study lies in the precision and speed of UAV-LiDAR for estimating individual tree structural parameters, together with its ability to non-destructively quantify biomass and carbon in heterogeneous and complex systems.

CRediT authorship contribution statement

Nilton Atalaya-Marin: Writing – original draft, Software, Methodology, Investigation, Formal analysis. **Teiser Sanchez-Fuentes:** Methodology, Investigation. **Malluri Goñas:** Validation, Supervision, Resources, Project administration, Data curation. **Daniel Tineo:** Validation, Supervision, Resources, Project administration, Data curation. **Victor H. Taboada-Mitma:** Validation, Supervision, Project administration. **Héctor Cabrera-Hoyos:** Visualization, Validation, Supervision, Project administration, Data curation. **JuanCarlos Cruz-Luis:** Validation, Supervision, Project administration. **Jorge J. Ganoza-Roncal:** Validation, Supervision, Project administration. **Darwin Gómez-Fernández:** Writing – review & editing, Validation, Software, Data curation.

Data availability statement

Upon reasonable request, the corresponding author will provide access to the data used to support the study's findings.

Declaration of generative AI and AI-assisted technologies in the writing process

During the preparation of this work the author used Chat GPT in order to improve readability and language. After using this tool, the authors reviewed and edited the content as needed and take full responsibility for the content of the publication.

Funding

This research was funded by the Instituto Nacional de Innovación Agraria (INIA) through an Investment Project with CUI No. 2472675 entitled: "Mejoramiento de los servicios de investigación y transferencia de tecnología agraria en la estación agraria experimental Baños del Inca en la localidad de Baños del Inca del distrito de Baños del Inca - provincia de Cajamarca - departamento de Cajamarca".

Declaration of competing interest

The authors declare that they have no known competing financial interests or personal relationships that could have appeared to influence the work reported in this paper.

Acknowledgements

The authors thank the Instituto Nacional de Innovación Agraria (INIA) through the Investment Project with CUI N°. 2472675 entitled: "Mejoramiento de los servicios de investigación y transferencia de tecnología agraria en la estación agraria experimental Baños del Inca en la localidad de Baños del Inca del distrito de Baños del Inca - provincia de Cajamarca - departamento de Cajamarca" which funded the execution of this research.

References

Almeida, D.R.A. de, Broadbent, E.N., Ferreira, M.P., Meli, P., Zambrano, A.M.A., Gorgens, E.B., Resende, A.F., de Almeida, C.T., do Amaral, C.H., Corte, A.P.D., Silva, C.A., Romanelli, J.P., Prata, G.A., de Almeida Papa, D., Stark, S.C., Valbuena, R., Nelson, B.W., Guillemot, J., Féret, J.B., Chazdon, R., Brancalion, P.H.S., 2021. Monitoring restored tropical forest diversity and structure through UAV-borne hyperspectral and lidar fusion. Remote Sens. Environ. 264, 112582. https://doi.org/10.1016/J.RSE.2021.112582.

Andrade, H.J., Segura, M., Somarriba, Eduardo, Villalobos, M., 2008. Valoración biofísica y financiera de la fijación de carbono por uso del suelo en fincas cacaoteras indígenas de Talamanca, Costa Rica.

Anguiano, J., Aguirre, J., Palma, J., 2013. Carbon sequestration in aboveground biomass of an agrosilvopastoral system (Cocos nucifera), (Leucaena leucocephala Var. Cunningham) and (Pennisetum purpureum) Cuba grass CT-115. Av. Invest. Agropecu.

Asigbaase, M., Dawoe, E., Lomax, B.H., Sjogersten, S., 2021. Biomass and carbon stocks of organic and conventional cocoa agroforests, Ghana. Agric. Ecosyst. Environ. 306, 107192. https://doi.org/10.1016/J.AGEE.2020.107192.

Asner, G.P., Mascaro, J., Muller-Landau, H.C., Vieilledent, G., Vaudry, R., Rasamoelina, M., Hall, J.S., van Breugel, M., 2012. A universal airborne LiDAR approach for tropical forest carbon mapping. Oecologia 168, 1147–1160. https://doi.org/10.1007/S00442-011-2165-Z/METRICS.

Atalaya-Marin, N., Goñas, M., Tineo, D., Chuquibala-Checan, B., Arce-Inga, M., Tarrillo, E., Alvarez-Robledo, Y.A., Tafur-Culqui, J., Cabrera-Hoyos, H., Gómez-Fernández, D., 2025. Integrating remote sensing and in-situ data to determine climate diversity and variability in cocoa systems in the provinces of Jaén and San Ignacio, Cajamarca (NW Perú). Trees Forests People 19, 100749. https://doi.org/10.1016/J.TFP.2024.100749.

Béjar-Martos, J.A., Rueda-Ruiz, A.J., Ogayar-Anguita, C.J., Segura-Sánchez, R.J., López-Ruiz, A., 2022. Strategies for the storage of large LiDAR datasets—A performance comparison. Remote Sens. 14, 2623. https://doi.org/10.3390/RS14112623, 14, 2623, 2022.

Benavides-Solrio, J. de D., Torres-García, J.G., Garnica, J.G.F., Mireles, M.A., Sánchez, A.R., 2021. Ecuaciones alométricas para estimar biomasa y carbono aéreos de Cedrela odorata L. en plantaciones forestales. Rev. Mex. Ciencias Farm. 12. https://doi.org/10.29298/RMCF.V12I65.791.

Cao, L., Liu, H., Fu, X., Zhang, Z., Shen, X., Ruan, H., 2019. Comparison of UAV LiDAR and digital aerial photogrammetry point clouds for estimating forest structural attributes in subtropical planted forests. Forests 10, 145. https://doi.org/10.3390/F10020145, 10, 145. 2019.

Clark, M.L., Clark, D.B., Roberts, D.A., 2004. Small-footprint lidar estimation of sub-canopy elevation and tree height in a tropical rain forest landscape. Remote Sens. Environ. 91, 68–89. https://doi.org/10.1016/J.RSE.2004.02.008.

Dantas, D., Rodrigues Pinto, L.O., de Castro Nunes Santos Terra, M., Calegario, N., Romarco de Oliveira, M.L., Dantas, D., Rodrigues Pinto, L.O., de Castro Nunes Santos Terra, M., Calegario, N., Romarco de Oliveira, M.L., 2020. Reduction of sampling intensity in forest inventories to estimate the total height of eucalyptus trees. Bosque (Valdivia) 41, 353–364. https://doi.org/10.4067/S0717-92002020000300353.

Deng, S., Xu, Q., Yue, Y., Jing, S., Wang, Y., 2024. Individual tree detection and segmentation from unmanned aerial vehicle-LiDAR data based on a trunk point distribution indicator. Comput. Electron. Agric. 218, 108717. https://doi.org/10.1016/J.COMPAG.2024.108717.

Duncanson, L., Kellner, J.R., Armston, J., Dubayah, R., Minor, D.M., Hancock, S., Healey, S.P., Patterson, P.L., Saarela, S., Marselis, S., Silva, C.E., Bruening, J., Goetz, S.J., Tang, H., Hofton, M., Blair, B., Luthcke, S., Fatoyinbo, L., Abernethy, K., Alonso, A., Andersen, H.E., Aplin, P., Baker, T.R., Barbier, N., Bastin, J.F., Biber, P., Boeckx, P., Bogaert, J., Boschetti, L., Boucher, P.B., Boyd, D.S., Burslem, D.F.R.P., Calvo-Rodriguez, S., Chave, J., Chazdon, R.L., Clark, D.B., Clark, D.A., Cohen, W.B., Coomes, D.A., Corona, P., Cushman, K.C., Cutler, M.E.J., Dalling, J.W., Dalponte, M., Dash, J., de-Miguel, S., Deng, S., Ellis, P.W., Erasmus, B., Fekety, P.A., Fernandez-Landa, A., Ferraz, A., Fischer, R., Fisher, A.G., García-Abril, A., Gobakken, T., Hacker, J.M., Heurich, M., Hill, R.A., Hopkinson, C., Huang, H., Hubbell, S.P., Hudak, A.T., Huth, A., Imbach, B., Jeffery, K.J., Katoh, M., Kearsley, E., Kenfack, D., Kljun, N., Knapp, N., Král, K., Krůček, M., Labrière, N., Lewis, S.L., Longo, M., Lucas, R.M., Main, R., Manzanera, J.A., Martínez, R.V., Mathieu, R., Memiaghe, H., Meyer, V., Mendoza, A.M., Monerris, A., Montesano, P., Morsdorf, F., Næsset, E., Naidoo, L., Nilus, R., O'Brien, M., Orwig, D.A., Papathanassiou, K., Parker, G., Philipson, C., Phillips, O.L., Pisek, J., Poulsen, J.R., Pretzsch, H., Rüdiger, C., Saatchi, S., Sanchez-Azofeifa, A., Sanchez-Lopez, N., Scholes, R., Silva, C.A., Simard, M., Skidmore, A., Stereńczak, K., Tanase, M., Torresan, C., Valbuena, R., Verbeeck, H., Vrska, T., Wessels, K., White, J.C., White, L.J.T., Zahabu, E., Zgraggen, C., 2022. Aboveground biomass density models for NASA's Global Ecosystem Dynamics Investigation (GEDI) lidar mission. Remote Sens. Environ. 270, 112845. https://doi.org/10.1016/J.RSE.2021.112845.

Fadil, S., Sebari, I., Moulay, M.A., El kadi, K.A., 2024. Modeling and spatialization of biomass and carbon stock using unmanned Aerial Vehicle Lidar (Lidar-UAV) metrics and forest inventory in cork oak forest of Maamora. Regional Sci Policy Practice 16, 100127. https://doi.org/10.1016/J.RSPP.2024.100127.

Fedorov, N., Bikbaev, I., Shirokikh, P., Zhigunova, S., Tuktamyshev, I., Mikhaylenko, O., Martynenko, V., Kulagin, A., Giniyatullin, R., Urazgildin, R., Komissarov, M., Belan, L., 2023. Estimation of carbon stocks of birch forests on abandoned arable lands in the cis-ural using unmanned aerial vehicle-mounted LiDAR camera. Forests 14, 2392. https://doi.org/10.3390/F14122392, 14, 2392 2023.

Fomekong, A.B., Momo Solefack, M.C., Mendi Anjah, G., Wouokoue Taffo, J.B., Kengne, O.C., Kenfack Feukeng, S.S., 2024. Site-species allometry equation for Theobroma cacao L. biomass estimation in agroforestry systems of Cameroon. Int. J. Ecol., 7096854 https://doi.org/10.1155/2024/7096854, 2024.

Food and Agriculture Organization of the United Nations [FAO], 2025. Agroforestería [WWW Document]. URL. https://www.fao.org/agroforestry/about-agroforestry/overview/es. (Accessed 1 August 2025).

Gobierno Regional de Cajamarca [GRC], 2012. Zonificación Ecológica y Económica: Base para el Ordenamiento Territorial del Departamento de Cajamarca.

Goñas, M., Rojas-Briceño, N.B., Gómez Fernández, D., Iliquín Trigoso, D., Atalaya Marin, N., Bravo, V.C., Díaz-Valderrama, J.R., Maicelo-Quintana, J.L., Oliva-Cruz, M., 2024. Economic profitability of carbon sequestration of fine-aroma Cacao agroforestry systems in Amazonas, Peru. Forests 15, 500. https://doi.org/10.3390/F15030500/S1.

Haneda, L.E., Brancalion, P.H.S., Valle, D., Silva, C.A., Gorgens, E.B., Prata, G.A., Kamimura, R.A., Gomes, S.H.M., Sanchez, A.K., Alves de Almeida, D.R., 2025. Edge effect impacts on forest structure and carbon stocks in REDD+ projects: an assessment in the Amazon using UAV-LiDAR. Forest Ecol. Manage. 585, 122646. https://doi.org/10.1016/J.FORECO.2025.122646.

Hirigoyen, A., Resquin, F., Cerrillo, R.N., Franco, J., Casnati, C.R., 2021. Stand biomass estimation methods for Eucalyptus grandis and Eucalyptus dunnii in Uruguay. Revista Bosque 42, 53–66. https://doi.org/10.4067/S0717-92002021000100053.

Jarahizadeh, S., Salehi, B., 2025. Advancing tree detection in forest environments: a deep learning object detector approach with UAV LiDAR data. Urban For. Urban Green. 105, 128695. https://doi.org/10.1016/J.UFUG.2025.128695.

Jucker, T., Caspersen, J., Chave, J., Antin, C., Barbier, N., Bongers, F., Dalponte, M., van Ewijk, K.Y., Forrester, D.I., Haeni, M., Higgins, S.I., Holdaway, R.J., Iida, Y., Lorimer, C., Marshall, P.L., Momo, S., Moncrieff, G.R., Ploton, P., Poorter, L., Rahman, K.A., Schlund, M., Sonké, B., Sterck, F.J., Trugman, A.T., Usoltsev, V.A., Vanderwel, M.C., Waldner, P., Wedeux, B.M.M., Wirth, C., Wöll, H., Woods, M., Xiang, W., Zimmermann, N.E., Coomes, D.A., 2017. Allometric equations for integrating remote sensing imagery into forest monitoring programmes. Glob. Change Biol. 23, 177–190. https://doi.org/10.1111/GCB.13388.

Ketterings, Q.M., Coe, R., Van Noordwijk, M., Ambagau', Y., Palm, C.A., 2001. Reducing uncertainty in the use of allometric biomass equations for predicting above-ground tree biomass in mixed secondary forests. Forest Ecol. Manage. 146, 199–209. https://doi.org/10.1016/S0378-1127(00)00460-6.

Kuyah, S., Muthuri, C., Wakaba, D., Cyamweshi, A.R., Kiprotich, P., Mukuralinda, A., 2024. Allometric equations and carbon sequestration potential of mango (Mangifera indica) and avocado (Persea americana) in Kenya. Trees Forests People 15, 100467. https://doi.org/10.1016/J.TFP.2023.100467.

Löhr, K., Aruqaj, B., Baumert, D., Bonatti, M., Brüntrup, M., Bunn, C., Castro-Nunez, A., Chavez-Miguel, G., Rio, M.L. Del, Hachmann, S., Muñoz, H.C.M., Ollendorf, F., Rodriguez, T., Rudloff, B., Schorling, J., Schuffenhauer, A., Schulte, I., Sieber, S., Tadesse, S., Ulrichs, C., Vogel, C., Weinhardt, M., 2021. Social cohesion as the missing link between natural resource management and peacebuilding: lessons from cocoa production in Côte d'ivoire and Colombia. Sustainability 13, 13002. https://doi.org/10.3390/SU132313002, 13, 13002 2021.

McGroddy, M.E., Daufresne, T., Hedin, L.O., 2004. Scaling of C:N:P stoichiometry in forests worldwide: implications of terrestrial redfield-type ratios. Ecology 85, 2390–2401. https://doi.org/10.1890/03-0351;CTYPE:STRING:JOURNAL.

McRoberts, R.E., Næsset, E., Liknes, G.C., Chen, Q., Walters, B.F., Saatchi, S., Herold, M., 2019. Using a finer resolution biomass map to assess the accuracy of a regional, map-based estimate of forest biomass. Surv. Geophys. 40, 1001–1015. https://doi.org/10.1007/S10712-019-09507-1/METRICS.

Miah, M.D., Islam, K.N., Kabir, M.H., Koike, M., 2020. Allometric models for estimating aboveground biomass of selected homestead tree species in the plain land Narsingdi district of Bangladesh. Trees Forests People 2, 100035. https://doi.org/10.1016/J.TFP.2020.100035.

Momo, S., Ploton, P., Sonké, B., Hackenberg, J., Griffon, S., de Coligny, F., Kamdem, N.G., Libalah, M., Mofack, G., Le Moguédec, G., Pélissier, R., Barbier, N., 2018. Using terrestrial laser scanning data to estimate large tropical trees biomass and calibrate allometric models: a comparison with traditional destructive approach. Methods Ecol. Evol. 9, 905–916. https://doi.org/10.1111/2041-210X.12933.

Neuville, R., Bates, J.S., Jonard, F., 2021. Estimating forest structure from UAV-mounted LiDAR point cloud using machine learning. Remote Sens. 13, 352. https://doi.org/10.3390/RS13030352, 13, 352 2021.

Ning, X., Li, F., Tian, G., Wang, Y., 2018. An efficient outlier removal method for scattered point cloud data. PLoS One 13, e0201280. https://doi.org/10.1371/JOURNAL.PONE.0201280.

Oliveira, C.P., Ferreira, R.L.C., da Silva, J.A.A., de Lima, R.B., Silva, E.A., da Silva, A.F., de Lucena, J.D.S., Dos Santos, N.A.T., Lopes, I.J.C., Pessoa, M.M. de L., de Melo, C.L.S.M.S., 2021. Modeling and spatialization of biomass and carbon stock using LiDAR metrics in tropical dry forest, Brazil. Forests 12, 473. https://doi.org/10.3390/F12040473, 12, 473, 2021.

Pati, P.K., Kaushik, P., Khan, M.L., Khare, P.K., 2022. Allometric equations for biomass and carbon stock estimation of small diameter woody species from tropical dry deciduous forests: support to REDD+. Trees Forests People 9, 100289. https://doi.org/10.1016/J.TFP.2022.100289.

Peynaud, E., Momo, S., 2024. Terrestrial LiDAR point cloud dataset of cocoa trees grown in agroforestry systems in Cameroon. Data Brief 53, 110108. https://doi.org/10.1016/J.DIB.2024.110108.

Pinedo, L.E., Ortega Quispe, K., Ccopi Trucios, D., Urquizo Barrera, J., Rios Chavarría, C., Pizarro Carcausto, S., Matos Calderon, D., Patricio Rosales, S., Rodríguez Cerrón, M., Ore Aquino, Z., Paz Monge, M., Castañeda Tinco, I., 2025. Estimation of height and aerial biomass in Eucalyptus globulus plantations using UAV-LiDAR. Trees Forests People 19, 100763. https://doi.org/10.1016/J.TFP.2024.100763.

Poggio, L., De Sousa, L.M., Batjes, N.H., Heuvelink, G.B.M., Kempen, B., Ribeiro, E., Rossiter, D., 2021. SoilGrids 2.0: producing soil information for the globe with quantified spatial uncertainty. Soil 7, 217–240. https://doi.org/10.5194/SOIL-7-217-2021.

Rajab, Y.A., Leuschner, C., Barus, H., Tjoa, A., Hertel, D., 2016. Cacao cultivation under diverse shade tree cover allows high carbon storage and sequestration without yield losses. PLoS One 11, e0149949. https://doi.org/10.1371/JOURNAL.PONE.0149949.

Schimalski, M.B., Mantas, V.M., Sothe, C., Wang, H., Li, D., Duan, J., Sun, P., 2024. ALS-Based, automated, single-tree 3D reconstruction and parameter extraction modeling. Forests 15, 1776. https://doi.org/10.3390/F15101776, 15, 1776, 2024.

Seidel, D., Stiers, M., Ehbrecht, M., Werning, M., Annighöfer, P., 2021. On the structural complexity of central European agroforestry systems: a quantitative assessment using terrestrial laser scanning in single-scan mode. Agrofor. Syst. 95, 669–685. https://doi.org/10.1007/S10457-021-00620-Y/FIGURES/7.

Servicio Nacional de Meteorología e Hidrología del Perú (SENAMHI), 2020. Mapa Climático del Perú [WWW Document]. URL. https://www.senamhi.gob.pe/?p=mapa-climatico-del-peru. (Accessed 19 March 2024).

Silva, C.A., Hudak, A.T., Vierling, L.A., Loudermilk, E.L., O'Brien, J.J., Hiers, J.K., Jack, S.B., Gonzalez-Benecke, C., Lee, H., Falkowski, M.J., Khosravipour, A., 2016. Imputation of individual longleaf pine (Pinus palustris Mill.) tree attributes from field and LiDAR data. Can. J. Rem. Sens. 42, 554–573. https://doi.org/10.1080/07038992.2016.1196582.

Su, R., Du, W., Ying, H., Shan, Y., Liu, Y., 2023. Estimation of aboveground carbon stocks in forests based on LiDAR and multispectral images: a case study of Duraer coniferous forests. Forests 14, 992. https://doi.org/10.3390/F14050992, 14, 992,2023.

Su, R., Du, W., Shan, Y., Ying, H., Rihan, W., Li, R., 2024. Aboveground carbon stock estimation based on backpack LiDAR and UAV multispectral imagery at the forest sample plot scale. Remote Sens. 16, 3927. https://doi.org/10.3390/RS16213927, 16, 3927,2024.

Tantrairatn, S., Pichitkul, A., Petcharat, N., Karaked, P., Ariyarit, A., 2025. Evaluating LiDAR technology for accurate measurement of tree metrics and carbon sequestration. MethodsX 14, 103237. https://doi.org/10.1016/J.MEX.2025.103237.

Thinley, J., Pickering, C., Ndehedehe, C., 2025. Modelling above ground biomass for a mixed-tree urban arboretum forest based on a LiDAR-derived canopy height model and field-sampled data. Geomatica 77, 100047. https://doi.org/10.1016/J.GEOMAT.2025.100047.

Vaglio, G., Puletti, N., Chen, Q., Corona, P., Papale, D., Valentini, R., 2016. Above ground biomass and tree species richness estimation with airborne lidar in tropical Ghana forests. Int. J. Appl. Earth Obs. Geoinf. 52, 371–379. https://doi.org/10.1016/J.JAG.2016.07.008.

White, J.C., Coops, N.C., Wulder, M.A., Vastaranta, M., Hilker, T., Tompalski, P., 2016. Remote sensing technologies for enhancing forest inventories: a review. Can. J. Rem. Sens. 42, 619–641. https://doi.org/10.1080/07038992.2016.1207484.

Zenner, E.K., Hibbs, D.E., 2000. A new method for modeling the heterogeneity of forest structure. Forest Ecol. Manage. 129, 75–87. https://doi.org/10.1016/S0378-1127(99)00140-1.

Zhao, X., Guo, Q., Su, Y., Xue, B., 2016. Improved progressive TIN densification filtering algorithm for airborne LiDAR data in forested areas. ISPRS J. Photogrammetry Remote Sens. 117, 79–91. https://doi.org/10.1016/J.ISPRSJPRS.2016.03.016.